HAL
archives-ouvertes.fr

Oligo-Miocene magnetostratigraphy and rock magnetism of the Xishuigou section, Subei (Gansu Province, western China) and implications for shallow inclinations in central Asia.

Stuart Gilder, Yan Chen, Sevket Sen

▶ To cite this version:

Stuart Gilder, Yan Chen, Sevket Sen. Oligo-Miocene magnetostratigraphy and rock magnetism of the Xishuigou section, Subei (Gansu Province, western China) and implications for shallow inclinations in central Asia.. Journal of Geophysical Research, American Geophysical Union, 2001, 106, pp.B12, 30505-30521. hal-00089760

HAL Id: hal-00089760
https://hal-insu.archives-ouvertes.fr/hal-00089760

Submitted on 29 Aug 2006

HAL is a multi-disciplinary open access archive for the deposit and dissemination of scientific research documents, whether they are published or not. The documents may come from teaching and research institutions in France or abroad, or from public or private research centers.

L'archive ouverte pluridisciplinaire **HAL**, est destinée au dépôt et à la diffusion de documents scientifiques de niveau recherche, publiés ou non, émanant des établissements d'enseignement et de recherche français ou étrangers, des laboratoires publics ou privés.

Oligo-Miocene magnetostratigraphy and rock magnetism of the Xishuigou section, Subei (Gansu Province, western China) and implications for shallow inclinations in central Asia

Stuart Gilder, **Yan Chen and Sevket Sen**

Laboratoire de Paléomagnétisme, Institut de Physique du Globe de Paris, Paris, France
Département des Sciences de la Terre, Université d'Orléans, Orléans, France
Laboratoire de Paléontologie du Muséum, Paris, France

Abstract

Magnetostratigraphy of 222 remanent directions together with late Oligocene to early Miocene mammal and charophyte paleontology suggest that 2179 m of the Xishuigou section (Subei, Gansu Province, China) were deposited from ~26 to ~19 Ma. Stratigraphic patterns of bulk susceptibility, anisotropy of magnetic susceptibility parameters, and natural and anhysteretic remanent magnetization intensities demonstrate that (1) faulting does not significantly affect the record, (2) sediment deposition was relatively continuous, (3) sediment source changed around 23 Ma, and (4) rapid uplift near Subei occurred at 21 Ma. Subei rotated 27° ± 5° counterclockwise with respect to the 20 Ma pole from the Eurasian synthetic apparent polar wander path. Folding and rotation of the section took place after 19 Ma. The paleolatitude of Subei is 14° less than at present and 19° ± 3° less than predicted from the reference pole. Both rock magnetic and paleomagnetic data sets suggest that the unusually low paleolatitude is the result of synsedimentary inclination shallowing, a phenomenon which has likely affected other paleomagnetic data from central Asia.

1. Introduction

With excellent exposures, extreme topography, and high strain rates, central Asia provides an exceptional opportunity to quantify geologic effects of intracontinental deformation related to the India-Asia collision. Past and present deformations have important consequences on climate change and impose a seismic threat to a growing population. Petroleum resources exceeding 1 billion barrels of oil that lie in the numerous foreland basins add an economic incentive to better understand how the region formed.

The indentor model of the India-Asia collision proposed by *Tapponnier and Molnar* [1977] provides a good starting point for understanding the paleogeographic evolution of the region.

The model suggests that northward subduction of the Indian plate has led to a combination of crustal thickening in, and lateral escape of, the relatively youthful and weaker blocks residing in Asia. Topographic highs such as the Tibetan Plateau and Heavenly Mountains (Tianshan) (Figure 1), which are bounded by active thrust faults, are products of crustal stacking related to compression. The dominant morphological feature in central Asia related to extrusion is the ~1500-km-long, N70°E trending Altyn Tagh fault, which divides the Tarim and Qaidam basins to the north and south, respectively (Figure 1). As the average elevation of the Tarim and Qaidam basins is ~1500 and ~3000 m, respectively, the fault forms a giant step with ~1500 m of vertical displacement. Several NW-SE trending mountain ranges, which are bordered by thrust faults, trend obliquely to the Altyn Tagh fault in the Qaidam basin. Because mountain ranges are absent in Tarim, north of Altyn Tagh, the fault likely accommodates left-lateral motion to compensate for the differential crustal shortening [*Meyer et al.*, 1998].

Qaidam's mountain ranges probably formed as ramp anticlines stacked upon crustal-scale thrust faults [*Tapponnier et al.*, 1990]. Sedimentary sequences deposited prior to tectonic exhumation often crop out in the thrust packages at the base of these ranges. One such sequence is found near Subei in western Gansu Province at the active front of the Tanghenan mountains, near the eastern terminus of the Altyn Tagh fault (Figure 1). There we performed a magnetostratigraphic study to constrain sedimentation rates and to better understand the tectonic history of this key area. We also employed a suite of rock magnetic experiments to detect potential environmental changes that occurred during sedimentation. Besides yielding tectonic information related to the Altyn Tagh fault, studying the paleomagnetism of the Subei section could provide welcome information on a highly debated controversy in the paleomagnetic community, namely, the origin of much lower than expected paleolatitudes (lower by >10°) observed throughout central Asia.

2. Geology and Sampling

Van der Woerd et al. [this issue] recently performed a detailed geologic study of the Subei area. The section described here lies within *Van der Woerd et al.*'s [this issue] drainage r8 (Xishuigou) (Figure 2), which is also referred to as Xigou by *Wang* [1997b]. This drainage trends north-south and incises Cenozoic fluvio-lacustrine sediments for over 5 km. To the south of the section, a major fault (F0) thrusts Paleozoic metamorphic rocks over the younger continental sediments. A synclinal fold axis where the beds change dip direction from north to south lies 400 m north of F0. We collected 538 paleomagnetic cores along a well-exposed, 2907-m-long (2179-m-thick) section beginning 15 m north of the fold axis. Ninety-six strike and/or dip measurements were made throughout the section, yielding a mean of N98°E, 48°S. Dips are fairly constant, suggesting that the units were not tilted during sedimentation (such as in a half graben) but that they were folded together after deposition. At 1088 m the section is cut by a small normal fault as well as by a bedding-parallel thrust fault (F″1) that, together, probably pinched away some of the sequence (Figure 2).

The sediments coarsen upward. The base consists of brick red poorly indurated mudstone, clay stone, and siltstone. Dominating the uppermost part of the section are 3- to 10-m-thick conglomerate beds, intercalated with small sandy lenses, that have well-rounded to slightly angular clasts measuring up to 1 m in diameter.

In the early 1930s, *Bohlin* [1937, 1942] studied the paleontology of the Subei region (then called Taban Buluk). From the diary of his expedition [*Bohlin*, 1945, p. 295] we are relatively sure that the fossils described in his memoir on the paleontology of Taban Buluk come from the same sequences that we sampled. *Bohlin* [1937] [see also *Wang*, 1997b, Appendix] broadly classified the fossils as Oligocene and Miocene. Today the fossils are much more tightly constrained in age, being typical of the upper Oligocene to lower Miocene. For example, *Tataromys grangeri* and the rodent *Yindirtemys woodi* are typical upper Oligocene species. Rabbits *Sinolagomys kansucnis*, *Desmatolagus shargaltensis*, and *D. paruidens* lived only during the lower Miocene. At Tiejianggou (Tiehchiangku), a stream valley 5 km west of Xishuigou, *Bohlin* [1946] identified the mammals *Sayimys obliquidens*, *Kansupithecus*, and *Proboscidi* sp. that *Wang* [1997a] and *Qiu and Qiu* [1995] have since correlated with European Neogene mammal zone MN3, which is calibrated by radiometric dating and magnetostratigraphy as lying between 18.0 and 20.5 Ma. X. Wang and W. Downs (personal communication, 2000) have recently found bones belonging to the Miocene deer *Amphimoschus artenensis*, which is restricted to the Orleanian. At the very base of our section we found a charophyte specimen identified as *Steftethamochara Huangjianensis*. This plant lived from the Eocene through the Oligocene with no known occurrence in the Miocene [*Lu and Luo*, 1990; H. Lu, personal communication, 1999]. Lizard bones that we found at 1218 m yielded no definitive age. In sum, the paleontologic data suggest that the base of the section lies in the upper Oligocene and that the 2179 m of sampled material spans the Oligo-Miocene boundary and continues into the lower Miocene.

We drilled two cores per horizon with an average distance between horizons of 8 m. Cores were oriented using standard magnetic and Sun compass techniques. The collection was divided into two parts, with one being measured at the Institut de Physique du Globe de Paris and the other at the Université d'Orléans.

3. Results

3.1. Magnetic Remanence

One sample per horizon was subjected to stepwise thermal demagnetization using at least 14 demagnetization steps. A second sample was demagnetized if the first yielded unstable or overprinted directions or if a polarity interval was defined by only one sample. In all, we measured the magnetic remanences of 368 samples with either a CTF Systems, Inc., superconducting quantum interference device (SQUID) magnetometer (Paris) or an AGICO, Inc., JR-5 spinner magnetometer (Orléans). The magnetic components of the samples were determined using principal component analysis [*Kirschvink*, 1980]. Magnetic characteristics were found to be laboratory independent.

Figure 3 shows representative *Zijderveld* [1967] plots. Many samples possess two magnetic components: one with variable but often north and down directions (in situ coordinates) at low to moderate temperatures (generally 200°C–500°C) that does not decay toward the origin and another at higher temperatures (generally $\geq$500°C) with shallow inclinations and north or south trending declinations (in situ coordinates) that does decay toward the origin. Other samples have a single component that is directed north and down (in situ coordinates) (Figure 3m), which is probably a recent overprint (geocentric axial dipole (GAD) direction is declination $D = 0°$ and inclination $I = 62.5°$; present-day field (PDF) is $D = 0.3°$, $I = 58.8°$). Remanent magnetizations of 222 samples were interpreted as having been acquired during

times of stable polarity, and 32 were interpreted as having been acquired during transitional times (Figures 3n and 3o). The remaining samples (n = 114) either possessed a PDF overprint or had unstable remanent directions.

of the 222 samples, 100 are of normal polarity and 122 are of reverse polarity (Figure 4 and Table 1). Slight changes in bedding attitudes do not permit the fold test to be applied with any significance. We did, however, sample an additional three sites ~1 km north of the section in steeply dipping fine-grained sediments that probably correlate with the lower part of the magnetostratigraphic sequence. Counting the magnetostratigraphic section as one site, the fold test based on the four sites is clearly positive, since the precision parameter increases 39 times from in situ to tilt-corrected coordinates (Table 1). For the magnetostratigraphic section the reversal test [*McFadden and McElhinny*, 1990] is negative at the 95% confidence level primarily because of differences in inclination values and because of small error ellipses that encompass the mean directions. The mean reversed polarity inclination is 8° shallower than that of normal polarity. This difference is most likely due to an unremoved overprint [*McElhinny et al.*, 1996; *Quidelleur and Courtillot*, 1996] that, because of the folding geometry and the present magnetic field direction, steepens the normal polarity directions and shallows the reversed polarity directions.

The overall mean tilt corrected direction is D = 350.2°, I = 43.8°, and radius within the 95% confidence limit, α_{95}, is 2.7°. After dividing the section into four equal lengths we noted that while there is no difference in inclination from bottom to top, there is a 15° difference in declination between the upper and lower halves (Table 1 and Figure 4).

3.2. Magnetostratigraphy

The magnetostratigraphy is shown in Figure 5, where 14 periods of reversed polarity (a through n) and 14 periods of normal polarity (1 through 14) are identified. While all intervals are represented by more than one sample, we note that two intervals (b and 11) are constrained by only two samples (Figures 3c and 3l), each lying in the same horizon, that were drilled a few centimeters from one another.

When correlating Subei's magnetostratigraphy with the reference global polarity timescale [*Berggren et al.*, 1995], we gave particular weight to matching the period of normal polarity spanning ~375 m of sediment (1 and 2 in Figure 5) to the long normal polarity chron (C6n) that lies within the time window constrained by the paleontological data (late Oligocene to early Miocene, 28.5–16.4 Ma). With this constraint we find a good match with the reference timescale starting at ~18.8 Ma (chron C5Er) until chron C6AAr.1n at 22.25 Ma. Fault F″1 lies below chron C6AAr.1n, and it is at this stage where fitting the various polarity intervals becomes less clear. Two correlations (I and II) are probable (Figures 5 and 6). Both assume that ~0.4 Myr (~120 m) is missing at the fault, which is likely due to the pinching out of a small slice of the section between F″1 and the normal fault, as shown in Figure 2. Correlation I yields a sedimentation rate of 36 cm kyr^{-1}, while correlation II has a sedimentation rate of 30 cm kyr^{-1}. We prefer II because I requires that the base of the section, which consists of much finer-grained sediments, has a higher sedimentation rate (43 cm kyr^{-1}) than the coarser-grained series at the top of the section (29 cm kyr^{-1}), which seems unlikely. If correlation II is correct, the Subei section considered here spans 7.3 Myr from ~26.1 to ~18.8 Ma. We note that the reference scale could lack reversed polarity interval b, and our study may thus indicate the existence of a new short-lived reversed polarity interval within chron C6n. The same could be true for the normal polarity interval 11 within chron C6Cn3r.

It should be questioned whether fault F″1 is a ramp fault, typical of thrust packages, potentially placing older sequences over younger ones; is it possible that the section below the fault is actually younger than 18.8 Ma? To address this, we note that (1) there is no fossil evidence for ages younger than the lower Miocene, (2) from below chron C5Er to the base of the upper Oligocene the reference scale is predominantly (60%) reversed polarity, consistent with our scale, (3) rock magnetic parameters (discussed in section 3.3) show no important step function across the fault, (4) the magnetostratigraphy above F″1 is quite different from that below F″1, and (5) the charophyte fossil should not be younger than Oligocene. We thus conclude that with the exception of a minor disturbance in the middle of the section, the series represents a relatively continuous rock record deposited during the late Oligocene (26.1 Ma) to early Miocene (18.8 Ma). Following *Agrinier et al.* [1999, Figure 2] we note that uncertainties in absolute age assignments based on magnetostratigraphic correlation reach 0.8 Ma in the Miocene.

3.3. Rock Magnetism

We first performed Curie point and isothermal remanent magnetization (IRM) experiments to characterize the magnetic mineralogy. Thermoremanent data show that 10 measured samples, including those near the bottom of the section, undergo a marked susceptibility decrease in the 500°C–580°C range, consistent with the presence of magnetite (Figures 7a–7d). IRM curves show that the samples contain a mineral whose coercivity is not saturated at fields of 0.9 T (Figures 7e–7h), which, together with unblocking temperatures of 680°C (Figure 3), is characteristic of hematite. The IRM curves also show a change in slope at fields <0.3 T, characteristic of magnetite. This change is more pronounced at the top of the section than at the bottom, suggesting greater magnetite abundances toward the top (Figures 7e–7h).

Low field susceptibility (k) of the samples treated by thermal demagnetization was measured after each demagnetization step. Viewed throughout the section, k varies rather systematically, with lower values at the base and higher ones toward the top (n = 256 samples; see Figure 8a). This pattern is mimicked by natural remanent magnetization intensities (JNRM) (Figure 8b). As the susceptibility of magnetite is ~1000 times greater than most minerals [*Collinson*, 1983], it is logical to suspect that the quantity of magnetite increases upward in the section. To test this hypothesis, we performed anhysteretic remanent magnetization (ARM) experiments using a continuous applied field of 0.1 mT and a peak maximum alternating field of 85 mT. Using these parameters, ARM intensities (JARM) should be controlled by magnetite rather than by hematite. We find that JARM closely resembles k and to a lesser extent (because of the superimposition of PDF and primary components), resembles JNRM (Figure 8). As the magnetic directions in most samples are similar at 550°C and 650°C (Figure 3), the lock-in time of the remanence in both minerals likely occurred during or very soon after deposition.

We then plotted k versus XARM (JARM/0.1 mT) (Figure 9), which, according to *King et al.* [1982, 1983], yields information related to magnetite grain size and abundance. King et al. found that points lying on the same line passing through the origin represent the same grain size, with steeper slopes corresponding to smaller grain sizes (however, note caveats by *Jackson et al.* [1988]). Points lying farther from the origin represent greater magnetite abundances. We divided the section into eight 275-m-thick parts and calculated the mean XARM and k for each part. These mean values are plotted together with the individual points in Figure 9. Interestingly, the means plot on the same line, with the lowest part (8/8) of the section lying closest to the origin and the uppermost part (1/8) lying farthest away. This

suggests that on average, the magnetite grain sizes are not growing larger but that the quantity of similarly sized magnetite particles generally increases upward.

3.4. Anisotropy of Magnetic Susceptibility

We measured the anisotropy of magnetic susceptibility (AMS) of 262 samples with a Kappabridge KLY-3 housed at the Université d'Orléans. The corrected anisotropy degree (P_j) [*Jelinek*, 1981] ranges from 1 to 11% with a mean and median of 4% (Figure 10a). P_j is independent of magnetite content (Figure 8c). This is also true for the shape parameter (T) and the normalized lineation (L) [*Hrouda*, 1982] (Figures 10b and 10c), which appear to vary with stratigraphic position. L increases from 1% at the base to 3% at 1600 m depth and then decreases to <1% at the top of the section. From the base (2179 m) to ~600 m, ellipsoids vary randomly, being either prolate (pencil-like, $T < 0$) or oblate (pancake-like, $T > 0$) with a mean near 0; above 600 m the form becomes generally oblate.

Figures 11a–11c show the principal maximum (k_1), intermediate (k_2), and minimum (k_3) directions of the ellipsoid axes. Bivariate statistics [*Henry and LeGoff*, 1995] are listed in Table 2, where it is suggested that when the section is cut into four equal length segments, the principal axis directions vary as a function of stratigraphic position. On average, k_3 inclinations are steepest at the top and shallowest at the base (Figure 11c); the opposite is true for k_2 inclinations (Figure 11b). The k_1 tilt-corrected directions generally parallel the strike of the fold axis, as is commonly found in folded sediments. Interestingly, the mean k_1 declinations imitate the pattern of the paleomagnetic declinations: both are rotated by similar amounts in the same sense above and below F″1 (Tables 1 and 2). This is a satisfying result in that whereas the picking of paleomagnetic directions can be seen as subjective, depending on which temperature steps are used and whether or not the best fit line segments are forced to the origin, there is no such degree of freedom with the AMS data. The good correlation between the two data sets thus gives further confidence in interpreting the paleomagnetic directions.

The deflection in k_3 inclinations from near bedding perpendicular in the upper conglomeratic beds toward the horizontal in the lower fine-grained units suggests that the original sedimentary fabric becomes progressively overprinted by tectonic strain. Such fabric development is well known both experimentally and theoretically [*Hrouda*, 1991; *Housen et al.*, 1993; *Kanamatsu et al.*, 1996; *Parés et al.*, 1999]. What is important here is that (1) the ratio of sedimentary to tectonic fabric is lithology dependent and (2) the girdle of k_3 inclinations is not symmetrically stretched out about the vertical but instead is shifted to the north, suggesting that deflection of the k_3 inclinations occurred during or after folding and faulting (Figure 11d).

4. Discussion

4.1. Depositional Environment

It has become increasingly clear over the past 2 decades that changes in rock magnetic properties observed in the sedimentary record can reflect shifts in climatic and/or tectonic regimes [*Thompson et al.*, 1980; *Verosub and Roberts*, 1995]. This also appears to be true for the Subei section (Figures 8a and 8c), where magnetite concentrations are low and constant from the base (2179 m) to ~1340 m depth, above which magnetite concentrations begin to

increase, as do the amplitudes of discreet peaks in k and to a lesser extent, as do JARM. Progressively greater magnetite abundances toward the top of the section could be attributed to (1) increased influx from a source rich in magnetite, (2) depth-dependent, postsedimentation destruction of original magnetite, and/or (3) a progressive pedogenic process (perhaps climate controlled) that favors magnetite precipitation. Because magnetite concentration and lithology correlate well and because paleomagnetic remanence directions in both magnetite and hematite are lithology independent, the second and third possibilities are improbable. Although sudden climatic events could account for pulses of concentrated magnetite, long-term changes in erosion rate should not control magnetite abundance because the ratio of magnetite to total eroded material would stay constant. Thus the first possibility is the most logical explanation, suggesting that magnetite-rich source rocks originally became exposed and eroded around 23.4 Ma and that their exposure and concomitant erosion amplified until at least 18.8 Ma.

While magnetite concentrations reflect source characteristics, AMS parameters can yield information related to sediment transport [*Rees*, 1964; *Kissel et al.*, 1998]. At Subei the AMS shape parameter (T) appears to vary systematically with depth (Figure 10b). From the base to ~620 m depth, bulk particle shapes are spherical on average, and then at 620 m (21 Ma; see Figure 5) they become notably oblate. Sphericity in the relatively fine grained part of the sequence likely reflects that the grains were relatively far traveled [*Krumbein*, 1941; *Kodama*, 1994; *Morris and Williams*, 1999]. The change to oblate ellipsoids occurs when the coarse conglomerate beds become dominant. Both the large clast sizes (>1 m) and oblate AMS shapes in these beds probably indicate that the source was in close proximity to the deposition center, as is consistent with both field and experimental data [*Krumbein*, 1941; *Kodama*, 1994; *Morris and Williams*, 1999]. We interpret this change at 21 Ma to reflect rapid uplift of the source near Subei that was possibly the Tanghenanshan. Thus the rock magnetic profiles can be interpreted to suggest that mountain building was active in the Subei area as early as 23–21 Ma. Other workers have also found evidence that active mountain building occurred in the region around this time, including (1) the commencement of unroofing found in apatite fission track dates along the central part of the Altyn Tagh fault (19 ± 1, 20 ± 2, and 22 ± 2 Ma [*Sobel et al.*, 2001]) and from the Tianshan (~24 Ma [*Hendrix et al.*, 1994]) and Kunlun ranges (25 to 13 Ma [*Sobel and Dumitru*, 1997]), (2) estimates of shortening rates from measured sections in the Tianshan by *Avouac et al.* [1993] that suggest a tectonic pulse occurred in the early to middle Miocene at 16 + 22/-9 Ma, and (3) the start of rapid continental sedimentation in the Tarim basin at ~22 Ma [*Métivier and Gaudemer*, 1997].

4.2. Regional Tectonics

The paleomagnetic direction for Subei is rotated 18° ± 4° counterclockwise with respect to the expected direction derived from the 20 Ma pole of the Eurasian synthetic apparent polar wander path (APWP) [*Besse and Courtillot*, 1991]. However, a 15° bedding-parallel rotation on F″1 is suggested by both the paleomagnetic and k_1 declinations, which are rotated by similar amounts in the same sense above and below the fault (Tables 1 and 2). Because the top part of the section is rotated less than the bottom part, it is likely that the whole section rotated as a single unit and then the section above F″1 back-rotated 15°. Thus the total tectonic rotation of the section is better represented by the mean direction calculated below F″1, which is D = 341.1°, I = 43.5°, α_{95} = 4.0°, n = 95 (Table 1). Both this direction and the overall mean direction are very similar to that found by *Rumelhart et al.* [1999] for Subei (D = 344.7°, I = 39.7°, α_{95} = 6.6°) from a more limited data set. A comparison of our n = 91 direction with the expected direction derived from the 20 Ma synthetic Eurasian pole suggests

that Subei has rotated 27° ± 5° counterclockwise. Taking the overall (n = 222) result into account and comparing this with its present position suggests that from 20 Ma to the present, Subei has moved north 14° (>1500 km) with respect to the present reference frame and 19° ± 3° (>2000 km) with respect to the 20 Ma synthetic Eurasian reference pole. The overall result was used in this latter comparison because inclination is not influenced by F″1 faulting (Table 1 and Figure 4).

Subei's low inclination poses a difficult problem in paleogeographic reconstructions of central Asia. This problem is not new; Late Jurassic through Tertiary inclinations from numerous studies throughout central Asia are systematically shallow with respect to the synthetic Eurasian APWP proposed by *Besse and Courtillot* [1991]. Several hypotheses have been proposed to explain this discrepancy, such as compaction-induced inclination shallowing, a tilted axial dipole, nondipolar geomagnetic field geometry, tectonic shortening, tectonic escape, remagnetization, and nonrigidity of the Eurasian plate [*Chen et al.*, 1991, 1992, 1993; *Pozzi and Feinberg*, 1991; *Thomas et al.*, 1993, 1994; *Westphal*, 1993; *Bazhenov et al.*, 1994; *Frost et al.*, 1995; *Cogné et al.*, 1995, 1999; *Chauvin et al.*, 1996; *Gilder et al.*, 1996; *Kodama and Tan*, 1997; *Halim et al.*, 1998]. The well-constrained age and small uncertainty of the Subei result significantly help to reduce the number of possible explanations.

The result suggests that Subei's northward motion since 20 Ma amounted to 7.5 cm yr^{-1}, or ~50% faster than the full convergence rate between the Indian and Eurasian plates [*Patriat and Achache*, 1984]. This implies that ~1000 km of extension occurred between Subei and India, which is a virtual impossibility. To explore the problem in more detail, we turned to the extensive central Asian paleomagnetic database, which contains 25 Late Jurassic to present paleomagnetic poles derived from central Asian localities lying north of the Tibetan Plateau (Figure 1 and Table 3). As previously noted by several workers, the poles are streaked out around small circles about the sampling localities, suggesting that their dispersion is best explained by local vertical axis block rotations. With this in mind, we used the small circle intersection method [*Besse and Courtillot*, 1991] to calculate an APWP for central Asia at 21.1, 44.2, 72.8, and 119.5 Ma (Figure 12 and Table 3). As seen in Figure 12, there exists a remarkable long-term stability in pole position. The poles appear to remain stationary until 3.5 Ma (which is the youngest available datum) [*Cogné et al.*, 1999] (Table 3). In paleogeographic terms, this suggests that a 3000-km swath of land resided at a stable paleolatitude, ~15° lower than at present, from ~130 to 3.5 Ma. Although the declination component appears to give a tectonically consistent picture, a tectonic solution of the paleolatitude data appears impossible because (1) plate velocity from 3.5 Ma to the present would be 43 cm yr^{-1}, far greater than any presently observed on the planet and (2) it would require displacements that well exceed those predicted from the India-Asia convergence rate. In sections 4.3 and 4.4 we explore the two most likely effects (geomagnetic field versus rock magnetism) that could account for the origin of the abnormally low central Asian paleolatitudes.

4.3. Geomagnetic Field

Both *Westphal* [1993] and *Chauvin et al.* [1996] proposed that a long-term, nondipole anomaly was present during the Tertiary in central Asia. This large-scale anomaly would be comparable in size to the Pacific Dipole Window [*Fisk*, 1931; *Doell and Cox*, 1972; *Merrill et al.*, 1996]. Persistent features in the geomagnetic field, especially during the last 5 Myr, have been advocated by several workers, including *Gubbins and Kelly* [1993], *Johnson and Constable* [1996], and *Kelly and Gubbins* [1997]. However, more recent work on the same

subject argues against long-lived, Pacific-Dipole-Window-sized anomalies [*Johnson and Constable*, 1997; *Carlut and Courtillot*, 1998], suggesting that earlier conclusions were biased by poor site and/or temporal coverage of the data. Moreover, *Kent and Smethurst* [1998] analyzed a worldwide database of 1536 Cenozoic and 1791 Mesozoic inclination observations and found that their frequency distributions were compatible with a time-averaged geomagnetic field that closely resembles a geocentric axial dipole. Thus, for central Asia it appears remotely possible that the shallow inclination problem arises from an aberration of the GAD hypothesis. No striking anomaly is presently indicated by the International Geomagnetic Reference Field direction and none is suggested by paleomagnetic inclinations from two Pleistocene basalt flows [*Otofuji et al.*, 1995].

4.4. Inclination Shallowing

If neither plate tectonics nor a geomagnetic field anomaly can explain the paleolatitude dilemma, could syndepositional or postdepositional effects that shallow remanent inclinations be responsible? At the latitudes of these basins (37°N–44°N), 15°–20° of shallowing is possible, depending on the amount of compaction [e.g., *Arason and Levi*, 1990]. However, several arguments exist against postdepositional compaction shallowing [*Gilder et al.*, 1996; *Cogné et al.*, 1999], which are further strengthened by the fabric analyses from the Subei section.

The relationships between sedimentation, magnetic remanence directions, and fabric acquisition have been much studied [*Rees*, 1961, 1964; *King and Rees*, 1966; *Owens*, 1974; *Jackson et al.*, 1991; *Hrouda*, 1991; *Tan and Kodama*, 1998; *Hrouda and Jezek*, 1999]. Concerning AMS directions, compaction-induced inclination shallowing should cause anisotropy degree (P_j) to increase and k_3 inclinations to rotate into the bedding normal to a greater extent than by sedimentation processes alone. Furthermore, rocks with high anisotropy and oblate AMS shapes ($T > 0$) should experience more shallowing than those with low anisotropy degrees and spherical ($T = 0$) or prolate ($T < 0$) shapes. These correlations are not observed in the Subei rocks; paleomagnetic inclinations are invariant through the section and show no correlation with P_j, T, or k_3 inclinations (Figures 10a, 10b, and 11c and Tables 1 and 2). On one hand, because bulk susceptibility correlates well with natural and anhysteretic remanent magnetization intensities (Figure 8), it can be inferred that the AMS signal is likely derived from the same grains that produce remanent magnetization directions, especially in the upper part of the section where magnetite concentration is greatest. On the other hand, understanding inclination shallowing from the AMS data is hindered by tectonic overprinting and systematic lithologic change. However, AMS shapes are markedly oblate in the upper part (Figure 10b), yet paleomagnetic inclinations there are indistinguishable from those lower down. Moreover, the more clay-rich rocks at the bottom of the section should be more susceptible to compaction shallowing than the coarse-grained layers on top, yet again no difference in inclination values is discerned.

Because north-south compression folded nearly all central Asian sediments about east-west trending fold axes, bedding-parallel shear could have physically rotated the magnetic grains [*Hrouda and Jezek*, 1999], which would have a large effect on magnetic inclinations. Shear rotation would tend to shallow inclinations on one flank of a fold while steepening them on the other, resulting in a negative fold test. This hypothesis is easily dismissed because most cases yield positive fold tests (see references in Table 3), including Subei. In conclusion, it appears that the remanent inclinations in the Subei section are lithology independent and that

significant postdepositional reorientation of them, either by compaction or by shear, is unlikely.

Finally, we note that laboratory redeposition experiments in running water on inclined beds can produce inclinations that are shallow by more than 30°, depending on current direction, magnetic field direction, original bedding slope, grain size, etc. [*King*, 1955; *Rees*, 1961, 1964, 1971; *Griffiths et al.*, 1962; *Hamilton and King*, 1964; *Rees and Woodall*, 1975]. These same experiments suggest that k_1 AMS directions are commonly oriented parallel to fluid flow or form a girdle distribution tilted downward into the flow direction due to imbrication. Inclination shallowing is especially marked when flow occurs in the magnetic field direction. For Subei the distribution of k_1 AMS directions is compatible with these observations assuming some of the k_1 directions were not completely reoriented during folding (Figure 11a). A great circle fit to all the data suggests that the mean flow direction was to the northeast during the Oligo-Miocene after accounting for the counterclockwise rotation. The girdle of k_1 AMS directions is tilted 21° ± 3° down to the south (tilt-corrected pole to great circle: D = 15.9°N, I = 69.0°, α_{95} = 3.2°). If this tilt resulted from a combination of original bedding error and imbrication, correcting the paleomagnetic inclination by 21° ± 3° brings the Subei result into full compatibility with the synthetic Eurasian APWP. Untilting the k_3 directions by 21° also brings them closer to bedding normal (Figure 11c). It thus appears that the best hypothesis to explain Subei's shallow paleolatitude is syndepositional shallowing of the remanent inclination.

5. Conclusions

We have presented the Oligo-Miocene magnetostratigraphy of the Xishuigou section from Subei, western Gansu Province, China. Our preferred magnetostratigraphic correlation with the reference polarity timescale of *Berggren et al.* [1995] that accounts for all paleontological constraints suggests that the 2179 m of sampled section spans from 26.1 to 18.8 Ma. Stratigraphic changes in rock magnetic parameters are attributed to combinations of sedimentary and tectonic influences. Rock magnetism also suggests that significant changes occurred in the sedimentary record at 23 and 21 Ma, which coincides with observed increases in sedimentation and tectonic shortening rates and apatite fission track cooling ages from the Altyn Tagh fault, the Tianshan and Kunlun mountains, and the Tarim basin. The Subei section rotated as a whole 27° ± 5° counterclockwise and was then cut by fault F″1, whence the upper part back-rotated ~15°. Folding and rotation occurred after 18.8 Ma. Subei's paleolatitude is 19° ± 3° shallower than expected; however, when local vertical axis block rotations are accounted for, its paleomagnetic pole is indistinguishable from 24 other central Asian poles spanning a 125-Myr time window. Our study suggests that a synsedimentary process shallowed Subei's remanent inclinations and that paleolatitude differences from 20 Ma to the present are primarily not a consequence of tectonic shortening, geomagnetic field anomaly, or compaction-induced shallowing, although much smaller proportions of these latter phenomena may have contributed. Because the drainage trends and sedimentary environments observed today in central Asia have likely remained constant since the Late Jurassic and because almost all of the data in Table 3 were produced from rock types similar to those for Subei, more rock magnetic data are needed to separate the influences of inclination shallowing and tectonic shortening. Future work should focus on rock types such as carbonates and volcanics, which are much less prone to inclination shallowing. It is also highly desirable to refine and expand on earlier laboratory experiments concerning the influence of running water on the recording of magnetic field directions.

Acknowledgments. This work is part of the Altyn Tagh Project supported by the French science organizations INSU and CNRS and the Ministry of Geology of China and headed by P. Tapponnier and Z. Q. Xu in 1996 and 1997. We thank Y. Gallet and Associate Editor T. Evans for critically reading the manuscript and providing useful criticisms and detailed comments. J. Besse, J. P. Cogné, V. Courtillot, W. Downs, B. Henry, M. LeGoff, M. G. Moreau, X. M. Wang, and two anonymous reviewers also contributed helpful advice. J. Van der Woerd kindly gave us an early version of his article. Paleomagnetic data were treated with the Paleomac program written by J. P. Cogné. This is IPGP contribution 1769.

Agrinier, P., Y. Gallet, and E. Lewin, On the age calibration of the geomagnetic polarity time scale, *Geophys. J. Int.*, *137*, 81–90, 1999.

Arason, P., and S. Levi, Models of inclination shallowing during sediment compaction, *J. Geophys. Res.*, *95*, 4481–4499, 1990.

Avouac, J. P., P. Tapponnier, M. Bai, H. You, and G. Wang, Active thrusting and folding along the northern Tien Shan and late Cenozoic rotation of the Tarim relative to Dzungaria and Kazakhstan, *J. Geophys. Res.*, *98*, 6755–6804, 1993.

Bazhenov, M. L., Cretaceous paleomagnetism of the Fergana Basin and adjacent ranges, central Asia: Tectonic implications, *Tectonophysics*, *221*, 251–267, 1993.

Bazhenov, M. L., H. Perroud, A. Chauvin, V. S. Burtman, and J. C. Thomas, Paleomagnetism of Cretaceous red beds from Tadzhikistan and Cenozoic deformation due to India-Eurasia collision, *Earth Planet. Sci. Lett.*, *124*, 1–18, 1994.

Berggren, W. A., D. V. Kent, C. C. Swisher, and M. P. Aubry, A revised Cenozoic geochronology and chronostratigraphy, in *Time Scales and Global Stratigraphic Correlation*, edited by W. A. Berggren et al., Geochronology, *Spec. Publ. SEPM Soc. Sediment. Geol.*, *54*, 129–212, 1995.

Besse, J., and V. Courtillot, Revised and synthetic apparent polar wander paths of the African, Eurasian, North American and Indian plates, and true polar wander since 200 Ma, *J. Geophys. Res.*, *96*, 4029–4050, 1991.

Bohlin, B., Oberoligozäne Säugetiere aus dem Shargaltein-Tal (western Kansu), *Palaeont. Sin., New Ser. C, Whole Ser.*, *107*, 1–66, 1937.

Bohlin, B., The fossil mammals from the Tertiary deposit of Taben-buluk, western Kansu, part I, Insectivora and Lagomorpha, *Palaeont. Sin., New Ser. C, Whole Ser., 123a*, 1–113, 1942.

Bohlin, B., Paleontological and geological researches in Mongolia and Kansu 1929–1933, in *Reports from the Scientific Expedition to the North-Western Provinces of China under the leadership of Dr. Sven Hedin, Publication 26: History of the Expedition in Asia 1927–1935, Part IV, General Reports of Travels and Field Work*, edited by F. Bergman et al., pp. 255–326, Thule, Stockholm, 1945.

Bohlin, B., The fossil mammals from the Tertiary deposit of Taben-buluk, western Kansu, part II, Simplicidentata, Carnivora, Artiodactyla, Perissodactyla, and Primates, *Palaeont. Sin., New Ser. C, Whole Ser., 123b*, 1–259, 1946.

Carlut, J., and V. Courtillot, How complex is the time-averaged geomagnetic field over the past 5 Myr?, *Geophys. J. Int., 134*, 527–544, 1998.

Chauvin, A., H. Perroud, and M. L. Bazhenov, Anomalous low paleomagnetic inclinations from Oligocene-lower Miocene red beds of the south-west Tien Shan, central Asia, *Geophys. J. Int., 126*, 303–313, 1996.

Chen, Y., et al., Paleomagnetic study of Mesozoic continental sediments along the northern Tien Shan (China) and heterogeneous strain in central Asia, *J. Geophys. Res., 96*, 4062–4082, 1991.

Chen, Y., J. P. Cogné, and V. Courtillot, New Cretaceous paleomagnetic poles from the Tarim basin, northwestern China, *Earth Planet. Sci. Lett., 114*, 17–38, 1992.

Chen, Y., V. Courtillot, J. P. Cogné, J. Besse, Z. Y. Yang, and R. Enkin, The configuration of Asia prior to the collision of India: Cretaceous paleomagnetic constraints, *J. Geophys. Res., 98*, 21,927–21,941, 1993.

Cogné, J. P., Y. Chen, V. Courtillot, F. Rocher, G. Q. Wang, M. X. Bai, and H. Z. You, A paleomagnetic study of Mesozoic sediments from Junggar and Turfan basins, NW China, *Earth Planet. Sci. Lett., 133*, 353–366, 1995.

Cogné, J. P., N. Halim, Y. Chen, and V. Courtillot, Resolving the problem of shallow magnetizations of Tertiary age in Asia: Insights from paleomagnetic data from the Qiangtang, Kunlun, and Qaidam blocks (Tibet, China), and a new hypothesis, *J. Geophys. Res., 104*, 17,715–17,734, 1999.

Collinson, D. W., *Methods in Rock Magnetism and Palaeomagnetism: Techniques and Instrumentation*, 503 pp., Chapman and Hall, New York, 1983.

Doell, R. R., and A. V. Cox, The Pacific geomagnetic secular variation anomaly and the question of lateral uniformity in the lower mantle, in *The Nature of the Solid Earth*, edited by E. C. Robertson, pp. 245–284, McGraw-Hill, New York, 1972.

Fisk, H. W., Isopors and isoporic movement, *Bull. Int. Geod. Geophys. Union, 8*, 280–292, 1931.

Frost, G. M., R. S. Coe, Z. F. Meng, Z. L. Peng, Y. Chen, V. Courtillot, G. Peltzer, P. Tapponnier, and J. P. Avouac, Preliminary Early Cretaceous paleomagnetic results from the Gansu Corridor, China, *Earth Planet. Sci. Lett., 129*, 217–232, 1995.

Gilder, S. A., X. X. Zhao, R. S. Coe, Z. F. Meng, V. Courtillot, and J. Besse, Paleomagnetism, tectonics and geology of the southern Tarim basin, northwestern China, *J. Geophys. Res., 101*, 22,015–22,031, 1996.

Griffiths, D. H., R. F. King, and A. I. Rees, The relevance of magnetic measurements on some fine grained silts to the study of their depositional process, *Sedimentology*, *1*, 134–144, 1962.

Gubbins, D., and P. Kelly, Persistent patterns in the geomagnetic field over the past 2.5 Myr, *Nature*, *365*, 829–832, 1993.

Halim, N., Contribution du paléomagnétisme à la compréhension de la tectonique post-collision entre Inde et Sibérie, Ph.D. dissertation, 239 pp., Inst. de Phys. du Globe de Paris, Paris, 1998.

Halim, N., J. P. Cogné, Y. Chen, R. Atasiei, J. Besse, V. Courtillot, S. Gilder, J. Marcoux, and R. L. Zhao, New Cretaceous and early Tertiary paleomagnetic results from Xining-Lanzhou basin, Kunlun and Qiangtang blocks, China: Implications on the geodynamic evolution of Asia, *J. Geophys. Res.*, *103*, 21,025–21,045, 1998.

Hamilton, N., and R. F. King, Comparison of the bedding errors of artificially and naturally deposited sediments with those predicted from a simple model, *Geophys. J. R. Astron. Soc.*, *8*, 370–374, 1964.

Hendrix, M. S., T. A. Dumitru, and S. A. Graham, Late Oligocene-early Miocene unroofing in the Chinese Tian Shan: An early effect of the India-Asia collision, *Geology*, *22*, 487–490, 1994.

Henry, B., and M. LeGoff, Application de l'extension bivariate de la statistique Fisher aux données d'anisotropie de susceptibilité magnétique: Intégration des incertitudes de mesure sur l'orientation des directions principales, *C. R. Acad. Sci., Ser. II*, *320*, 1037–1042, 1995.

Housen, B. A., C. Richter, and B. A. van der Pluijm, Composite magnetic anisotropy fabrics: Experiments, numerical models, and implications for the quantification of rock fabrics, *Tectonophysics*, *220*, 1–12, 1993.

Hrouda, F., Magnetic anisotropy of rocks and its application in geology and geophysics, *Geophys. Surv.*, *5*, 37–82, 1982.

Hrouda, F., Models of magnetic anisotropy variations in sedimentary thrust sheets, *Tectonophysics*, *185*, 203–210, 1991.

Hrouda, F., and J. Jezek, Magnetic anisotropy indications of deformations associated with diagenesis, in *Paleomagnetism and Diagenesis in Sediments*, edited by D. H. Tarling and P. Turner, *Geol. Soc. Spec. Publ.*, *151*, 127–137, 1999.

Jackson, M., W. Gruber, J. Marvin, and S. K. Banerjee, Partial anhysteretic remanence and its anisotropy; applications and grain size dependence, *Geophys. Res. Lett.*, *15*, 440–443, 1988.

Jackson, M. J., S. K. Banerjee, J. A. Marvin, R. Lu, and W. Gruber, Detrital remanence, inclination errors, and anhysteretic remanence anisotropy: Quantitative model and experimental results, *Geophys. J. Int.*, *104*, 95–103, 1991.

Jelinek, V., Characterization of the magnetic fabrics of rocks, *Tectonophysics*, *79*, 63–67, 1981.

Johnson, C., and C. Constable, Paleosecular variation recorded by lava flows over the last 5 Myr, *Philos. Trans. R. Soc. London, Ser. A, 354*, 89–141, 1996.

Johnson, C., and C. Constable, The time-averaged geomagnetic field: Global and regional biases for 0–5 Ma, *Geophys. J. Int.*, *131*, 643–666, 1997.

Kanamatsu, T., E. Herroro-Bervera, A. Taira, S. Saito, J. Ashi, and A. S. Furumoto, Magnetic fabric development in the tertiary accretionary complex in the Boso and Miuia Peninsulas of central Japan, *Geophys Res. Lett.*, *23*, 471–474, 1996.

Kelly, P., and D. Gubbins, The geomagnetic field over the past 5 million years, *Geophys. J. Int.*, *128*, 315–330, 1997.

Kent, D. V., and M. A. Smethurst, Shallow bias of paleomagnetic inclinations in the Paleozoic and Precambrian, *Earth Planet. Sci. Lett.*, *160*, 391–402, 1998.

King, J. W., S. K. Banerjee, J. Marvin, and Ö. Özdemir, A comparison of different magnetic methods for determining the relative grain size of magnetite in natural materials: Some results from lake sediments, *Earth Planet. Sci. Lett.*, *59*, 404–419, 1982.

King, J. W., S. K. Banerjee, and J. Marvin, A new rock-magnetic approach to selecting sediments for geomagnetic paleointensity studies: Application to paleointensity for the last 4000 years, *J. Geophys. Res.*, *88*, 5911–5921, 1983.

King, R. F., The remanent magnetism of artificially deposited sediments, *Mon. Not. R. Astron. Soc., Geophys. Suppl.*, *7*, 115–134, 1955.

King, R. F., and A. I. Rees, Detrital magnetism in sediments: An examination of some theoretical models, *J. Geophys. Res.*, *71*, 561–571, 1966.

Kirschvink, J. L., The least-square line and plane and the analysis of paleomagnetic data, *Geophys. J. R. Astron. Soc.*, *62*, 699–712, 1980.

Kissel, C., C. Laj, A. Mazaud, and T. Dokken, Magnetic anisotropy and environmental changes in two sedimentary cores from the Norwegian Sea and the North Atlantic, *Earth Planet. Sci. Lett.*, *164*, 617–626, 1998.

Kodama, K. P., and X. Tan, Central Asian inclination anomalies: Possible inclination shallowing in red beds? (abstract), *Eos Trans. AGU*, *78*(46), Fall Meet. Suppl., F174, 1997.

Kodama, Y., Experimental study of abrasion and its role in producing downstream fining in gravel-bed rivers, *J. Sediment. Res., Sect. A*, *64*, 76–85, 1994.

Krumbein, W. C., The effects of abrasion on the size, shape and roundness of rock fragments, *J. Geol.*, *64*, 482–520, 1941.

Li, Y. P., Z. K. Zhang, M. McWilliams, R. Sharps, Y. J. Zhai, Y. A. Li, Q. Li, and A. Cox, Mesozoic paleomagnetic results of the Tarim craton: Tertiary relative motion between China and Siberia, *Geophys. Res. Lett.*, *15*, 217–220, 1988.

Lu, H. N., and Q. X. Luo, Fossil charophytes from the Tarim basin, Xinjiang, in *Tarim Basin Charophyte Fossils*, edited by H. N. Lu and Q. X. Luo, pp. 177–201, Sci. Technol. Publ. House, Beijing, 1990.

McElhinny, M. W., P. L. McFadden, and R. T. Merrill, The time-averaged paleomagnetic field 0–5 Ma, *J. Geophys. Res.*, *101*, 25,007–25,028, 1996.

McFadden, P. L., and M. W. McElhinny, Classification of the reversal test in palaeomagnetism, *Geophys. J. Int.*, *130*, 725–729, 1990.

Merrill, R. T., M. W. McElhinny, and P. L. McFadden, *The Magnetic Field of the Earth, Int. Geophys. Ser.*, vol. 63, 531 pp., Academic, San Diego, Calif., 1996.

Métivier, F., and Y. Gaudemer, Mass transfer between eastern Tien Shan and adjacent basins (central Asia): Constraints on regional tectonics and topography, *Geophys. J. Int.*, *128*, 1–17, 1997.

Meyer, B., P. Tapponnier, L. Bourjot, F. Métivier, Y. Gaudemer, G. Peltzer, S. M. Guo, and Z. T. Chen, Crustal thickening in Gansu-Qinghai, lithospheric mantle subduction, and oblique, strike-slip controlled growth of the Tibet Plateau, *Geophys. J. Int.*, *135*, 1–47, 1998.

Morris, P. H., and D. J. Williams, A worldwide correlation for exponential bed particle size variation in subaerial aqueous flows, *Earth Surf. Processes Landforms*, *24*, 835–847, 1999.

Otofuji, Y., T. Itaya, H. C. Wang, and S. Nohda, Palaeomagnetism and K-Ar dating of Pleistocene volcanic rocks along the Altyn Tagh fault, northern border of Tibet, *Geophys. J. Int.*, *120*, 367–374, 1995.

Owens, W. H., Mathematical model studies on factors affecting the magnetic anisotropy of deformed rocks, *Tectonophysics*, *24*, 115–131, 1974.

Parés, J. M., B. A. van der Pluijm, and J. Dinarès-Turell, Evolution of magnetic fabrics during incipient deformation of mudrocks (Pyrenees, northern Spain), *Tectonophysics, 307*, 1–14, 1999.

Patriat, P., and J. Achache, India-Eurasia collision chronology has implications for crustal shortening and driving mechanism of plates, *Nature*, *311*, 615–621, 1984.

Pozzi, J. P., and H. Feinberg, Paleomagnetism in the Tajikistan: Continental shortening of European margin in the Pamirs during Indian Eurasian collision, *Earth Planet. Sci. Lett.*, *103*, 365–378, 1991.

Qiu, Z., and Z. Qiu, Chronological sequence and subdivisions of Chinese Neogene mammalian faunas, *Paleogeogr. Palaeoclimatol. Palaeoecol.*, *166*, 41–70, 1995.

Quidelleur, X., and V. Courtillot, On low degree spherical harmonic models of paleosecular variation, *Phys. Earth Planet. Inter.*, *95*, 55–77, 1996.

Rees, A. I., The effect of water currents on the magnetic remanence and anisotropy of susceptibility of some sediments, *Geophys. J. R. Astron. Soc.*, *5*, 235–251, 1961.

Rees, A. I., Measurements of the natural remanent magnetism and anisotropy of susceptibility of some Swedish glacial silts, *Geophys. J. R. Astron. Soc.*, *8*, 356–369, 1964.

Rees, A. I., The magnetic fabric of a sedimentary rock deposited on a slope, *J. Sediment. Petrol.*, *41*, 307–309, 1971.

Rees, A. I., and W. A. Woodall, The magnetic fabric of some laboratory-deposited sediments, *Earth Planet. Sci. Lett.*, *25*, 121–130, 1975.

Rumelhart, P. E., A. Yin, E. Cowgill, R. Butler, Z. Qing, and X. F. Wang, Cenozoic vertical axis rotation of the Altyn Tagh fault system, *Geology*, *27*, 819–822, 1999.

Sobel, E. R., and T. A. Dumitru, Thrusting and exhumation around the margins of the western Tarim basin during the India-Asia collision, *J. Geophys. Res.*, *102*, 5043–5063, 1997.

Sobel, E. R., N. Arnaud, M. Jolivet, B. D. Ritts, and M. Brunel, Jurassic to Cenozoic exhumation history of the Altyn Tagh range, NW China constrained by $^{40}Ar/^{39}Ar$ and apatite fission track thermochronology, in *Paleozoic and Mesozoic Tectonic Evolution of Central and Eastern Asia: From Continental Assembly to Intracontinental Deformation*, edited by M. S. Hendrix and G. A. Davis, *Mem. Geol. Soc. Am.*, *194*, in press, 2001.

Tan, X. D., and K. P. Kodama, Compaction-corrected inclinations from southern California Cretaceous marine sedimentary rocks indication no paleolatitudinal offset for the Peninsula Ranges terrane, *J. Geophys. Res.*, *103*, 27,169–27,192, 1998.

Tapponnier, P., and P. Molnar, Active faulting and tectonics in China, *J. Geophys. Res.*, *82*, 2905–2930, 1977.

Tapponnier, P., et al., Active thrusting and folding in the Qi Lian Shan, and decoupling between the upper crust and mantle in northeastern Tibet, *Earth Planet. Sci. Lett.*, *97*, 382–403, 1990.

Thomas, J. C., H. Perroud, P. R. Cobbold, M. L. Bazhenov, V. S. Burtman, A. Chauvin, and E. Sadybakasov, A paleomagnetic study of Tertiary formations from the Kyrgyz Tien-Shan and its tectonic implications, *J. Geophys. Res.*, *98*, 9571–9589, 1993.

Thomas, J. C., A. Chauvin, D. Gapais, M. L. Bazhenov, H. Perroud, P. R. Cobbold, and V. S. Burtman, Paleomagnetic evidence for Cenozoic block rotations in the Tadjik depression (central Asia), *J. Geophys. Res.*, *99*, 15,141–15,160, 1994.

Thompson, R., J. Bloemendal, J. A. Dearing, F. Oldfield, T. A. Rummery, J. C. Stober, and G. M. Turner, Environmental applications of magnetic measurements, *Science*, *207*, 481–486, 1980.

Van der Woerd, J., P. Tapponnier, X. W. Xu, B. Meyer, F. J. Ryerson, and A. S. Meriaux, Rapid active thrusting and river incision along the northwestern rangefront of the Tanghenanshan (western Gansu, China), *J. Geophys. Res.*, this issue.

Verosub, K. L., and A. P. Roberts, Environmental magnetism: Past, present, and future, *J. Geophys. Res.*, *100*, 2175–2192, 1995.

Wang, B., The mid-Tertiary Ctenodactylidae (Rodentia, Mammalia) of eastern and central Asia, *Bull. Am. Mus. Nat. Hist., 234*, 1–88, 1997a.

Wang, E., Displacement and timing along the northern strand of the Altyn Tagh fault zone, northern Tibet, *Earth Planet. Sci. Lett., 150*, 55–64, 1997b.

Westphal, M., Did a large departure from the geocentric axial dipole hypothesis occur during the Eocene? Evidence from the magnetic polar wander path of Eurasia, *Earth Planet. Sci. Lett., 117*, 15–28, 1993.

Zijderveld, J. D. A., AC demagnetization of rocks-analysis of results, in *Methods in Paleomagnetism*, edited by D. W. Collinson, K. M. Creer, and S. K. Runcorn, pp. 254–286, Elsevier Sci., New York, 1967.

Y. Chen, Département des Sciences de la Terre, Université d'Orléans, B.P. 6759, F-45067 Orléans Cedex 02, France. (Yan.Chen@univ-orleans.fr)

S. Gilder, Laboratoire de Paléomagnétisme, Institut de Physique du Globe de Paris, 4 place Jussieu, F-75252 Paris Cedex 05, France. (gilder@ipgp.jussieu.fr)

S. Sen, Laboratoire de Paléontologie du Muséum, 8 rue Buffon, F-75005 Paris, France. (Sen@mnhn.fr)

Figures

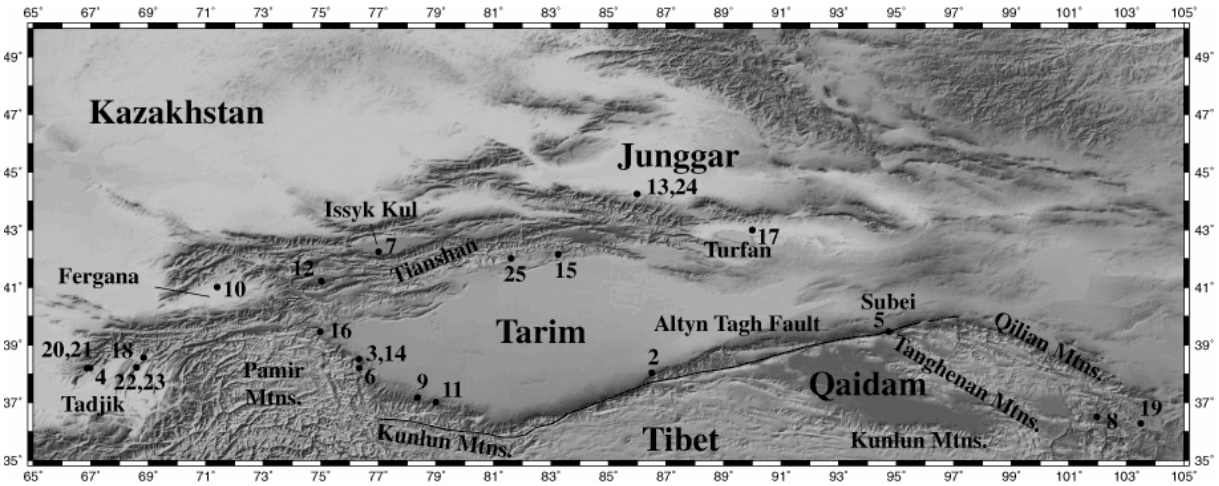

Figure 1. Topographic map of central Asia showing major basins and mountain ranges. Numbers correspond to paleomagnetic sampling sites in Table 3.

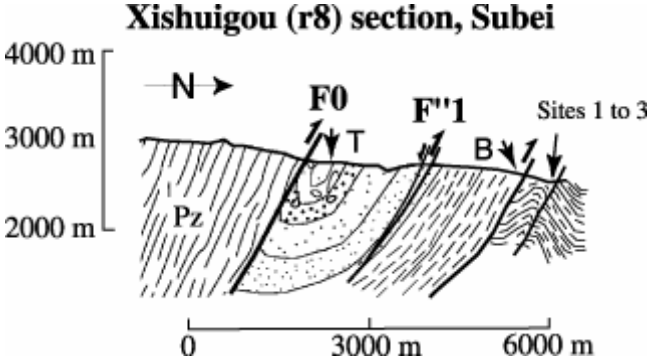

Figure 2. Simplified cross section of the Xishuigou (r8) section at Subei [after *Van der Woerd et al.*, this issue]. Arrows show top (T) and bottom (B) of magnetostratigraphic section from this study. Transition from fine- to coarse-grained sediments is schematic. Pz represents Paleozoic metamorphic rocks.

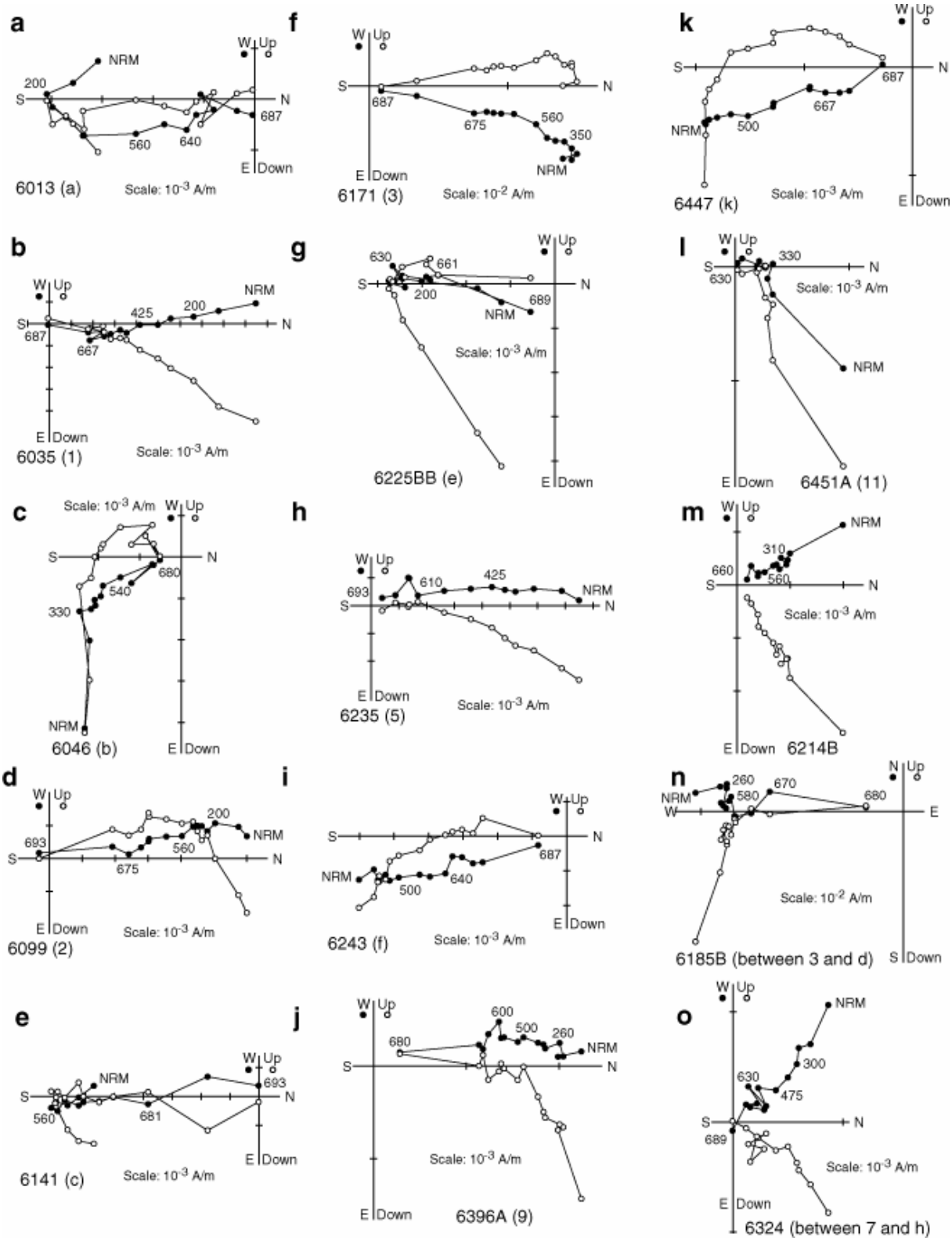

Figure 3. *Zijderveld* [1967] plots from thermal demagnetization experiments (all in in situ coordinates). Numbers next to demagnetization steps are temperatures in degrees Celsius; natural remanent magnetization (NRM) is the room temperature step. Numbers at bottom left of plots are sample numbers (6001 is top of section, 6545 is bottom); numbers and letters in parentheses correspond to polarity sequences shown in Figure 5.

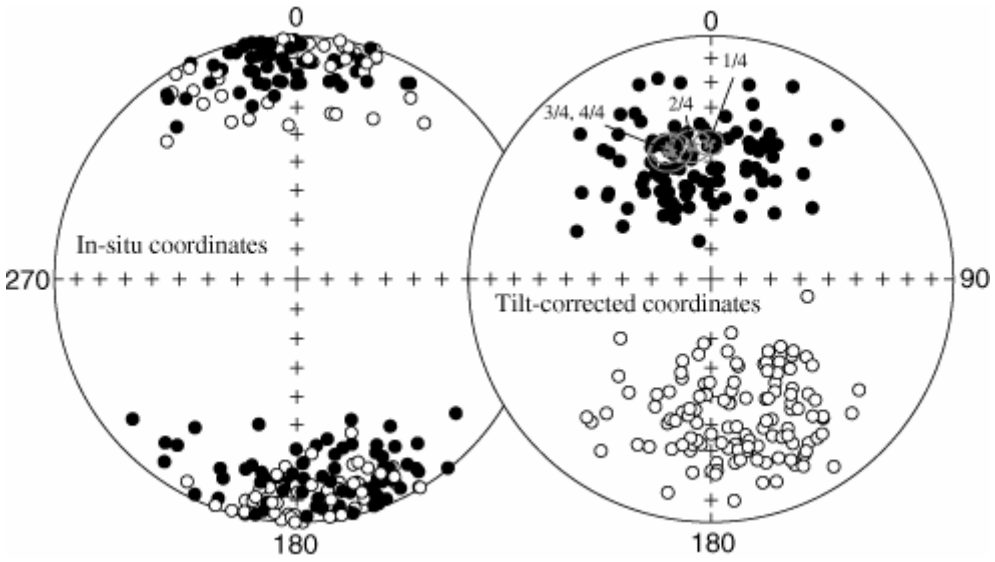

Figure 4. Stereonet plot of 222 magnetization directions used to constrain the magnetostratigraphy shown in Figure 5. Open (solid) circles are projected on the upper (lower) hemisphere. Stars and 95% confidence ellipses are mean values of each quarter of the section (1/4 is top; 4/4 is bottom) (data from Table 1).

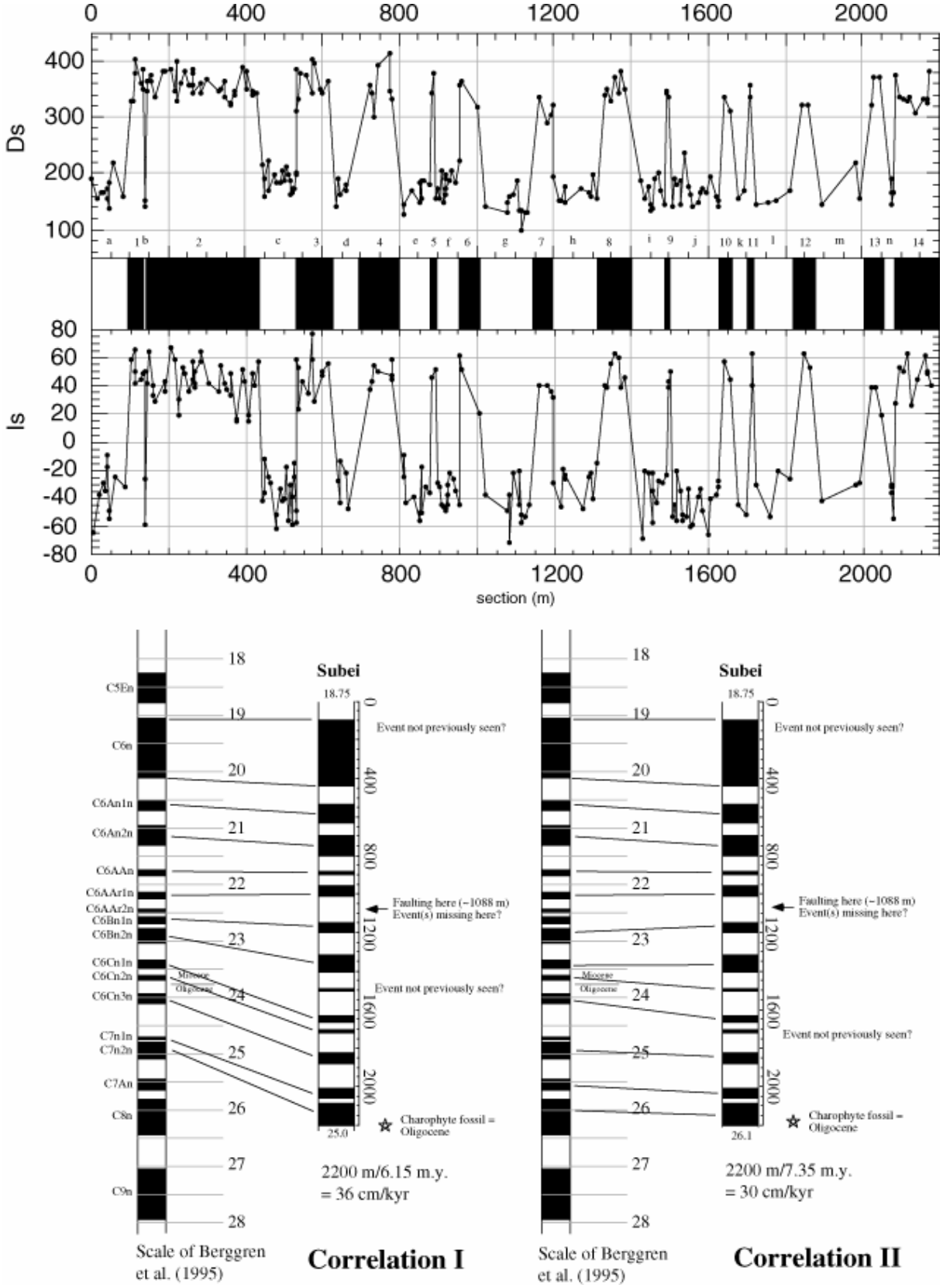

Figure 5. (top) Magnetic polarity scale of the Xishuigou section, Subei, and (bottom) two correlations with the reference scale of *Berggren et al.* [1995]. Normal polarity reference chrons are listed on left scale.

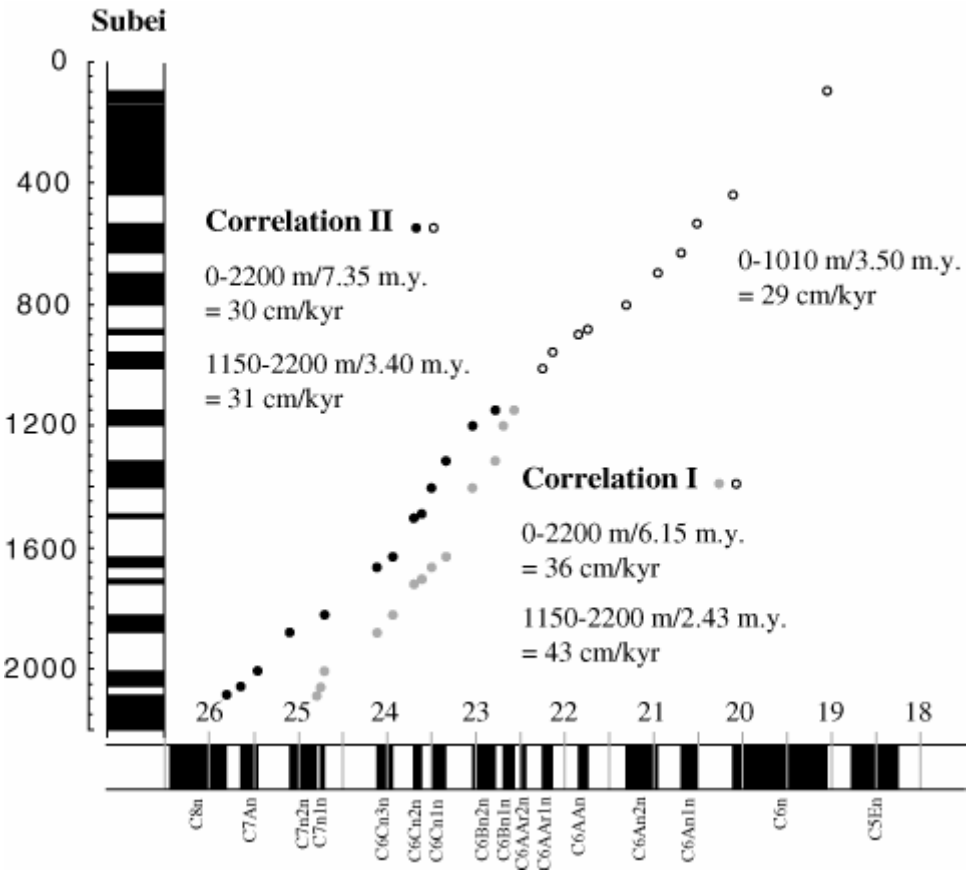

Figure 6. Age versus depth plot of the Xishuigou section, Subei, using data and correlations from Figure 5.

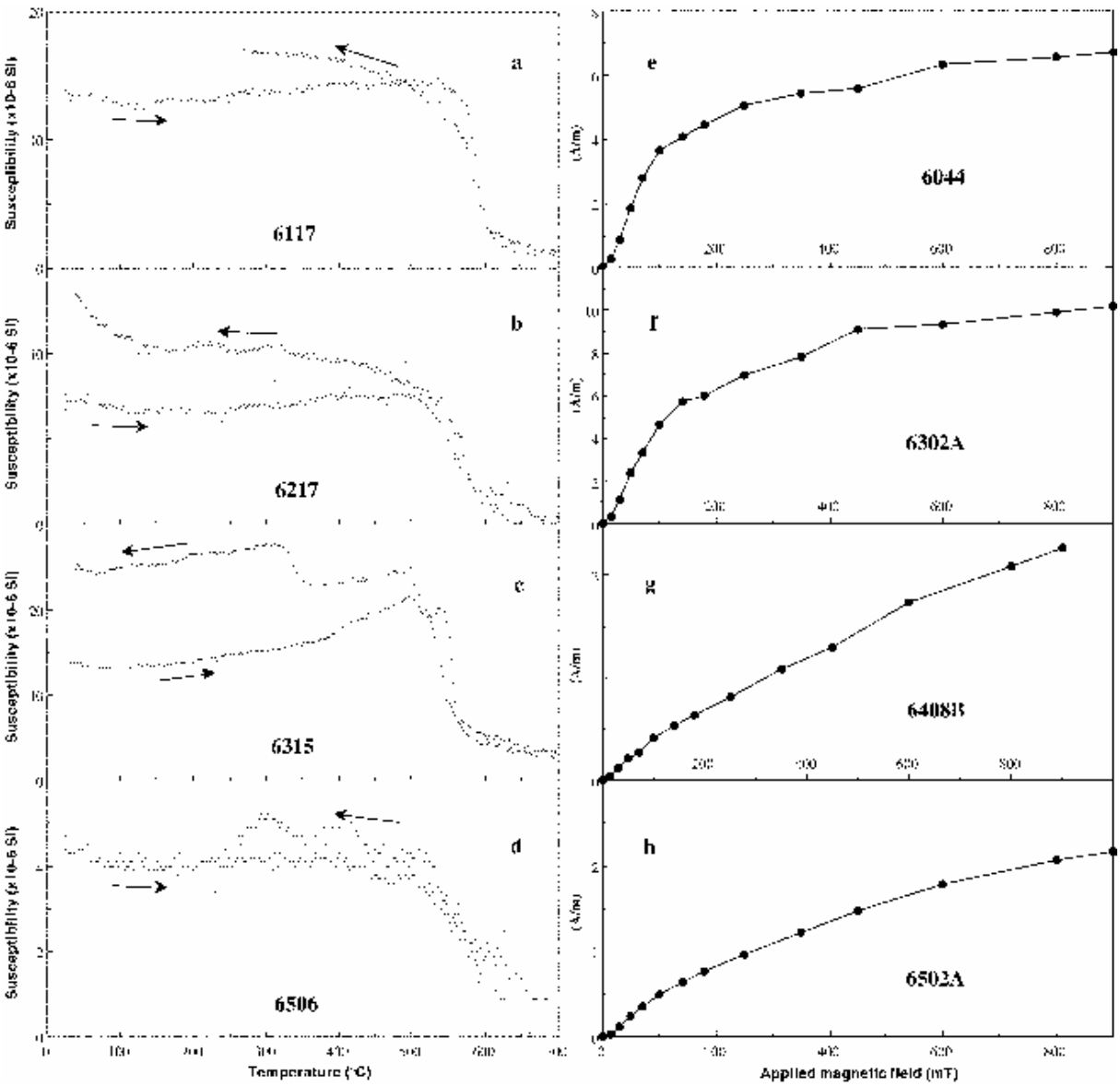

Figure 7. (a–d) Magnetic susceptibility versus temperature. (e–h) Isothermal remanent magnetization plots. Note that sample 6001 is at the top of the section and sample 6546 is at the bottom.

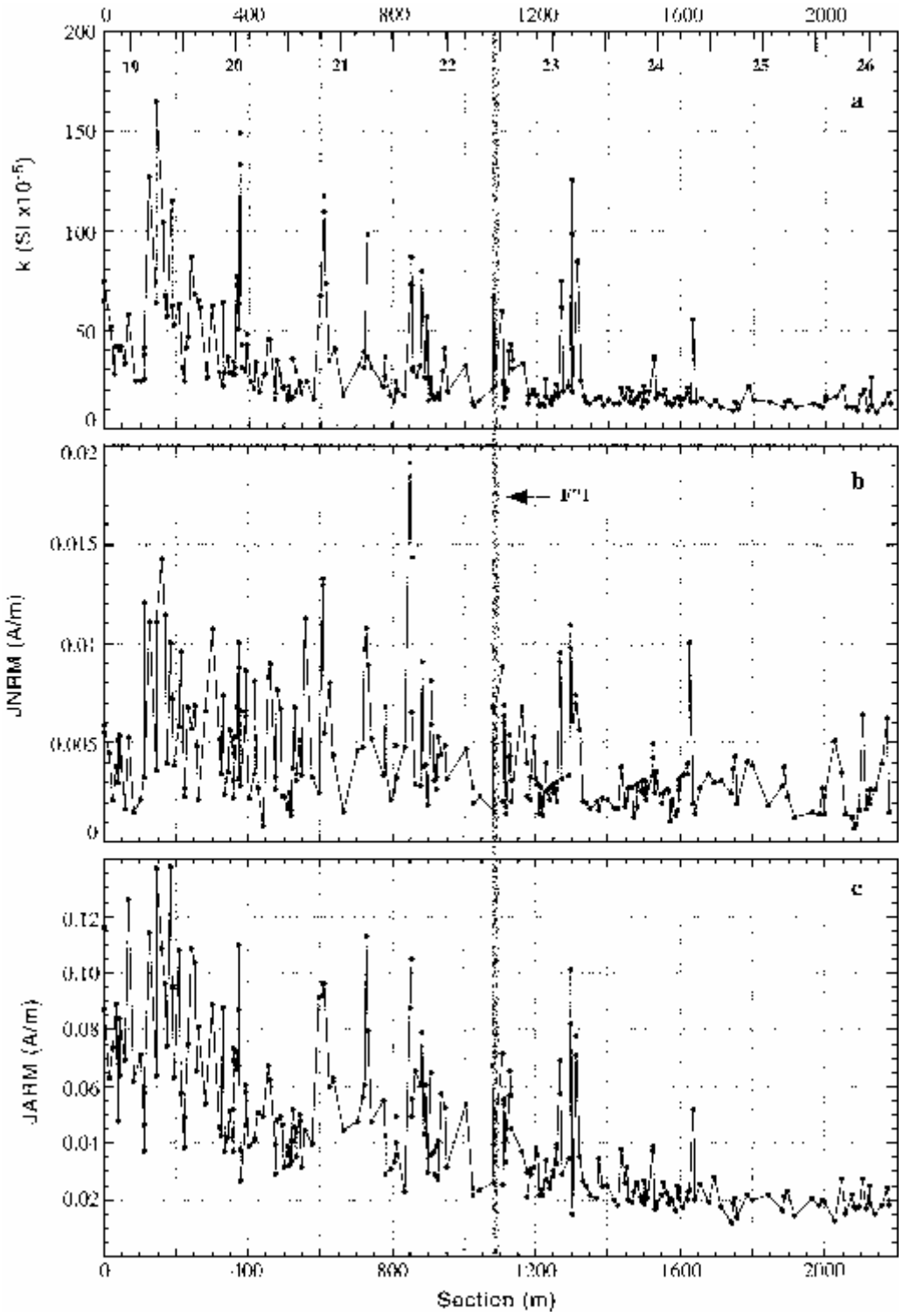

Figure 8. (a) Bulk susceptibility (*k*), (b) NRM intensity (JNRM), and (c) anhysteretic remanent magnetization intensity (JARM) plotted against depth (0 is top; 2179 m is bottom). Scale in Ma from correlation II of Figure 5 is provided in Figure 8a.

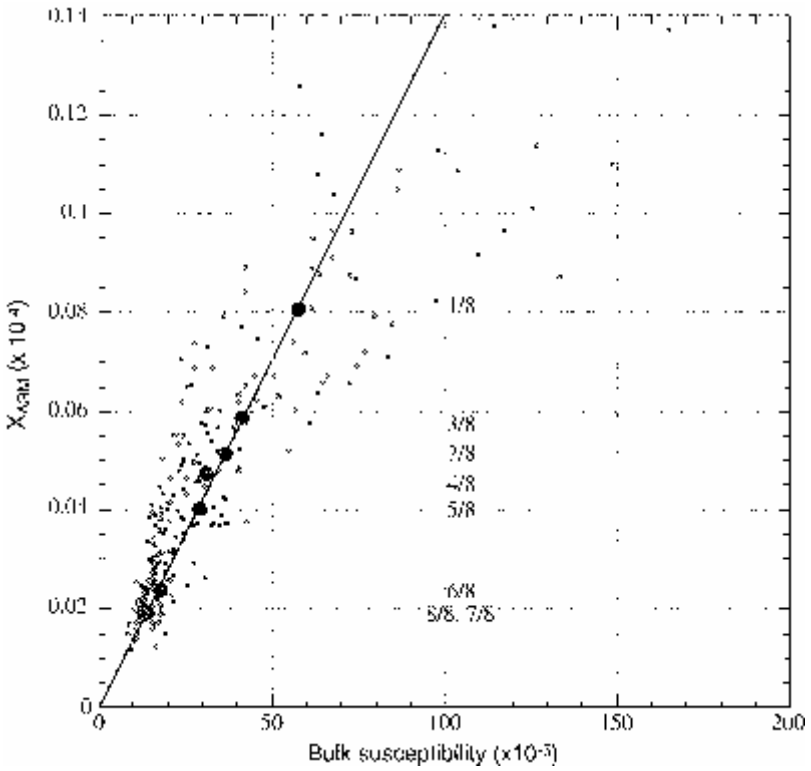

Figure 9. Normalized anhysteretic remanent magnetization intensity plotted against *k* (open circles). Solid circles are mean values of each eighth of the section (1/8 is top; 8/8 is bottom). Note that mean values lie on the same slope.

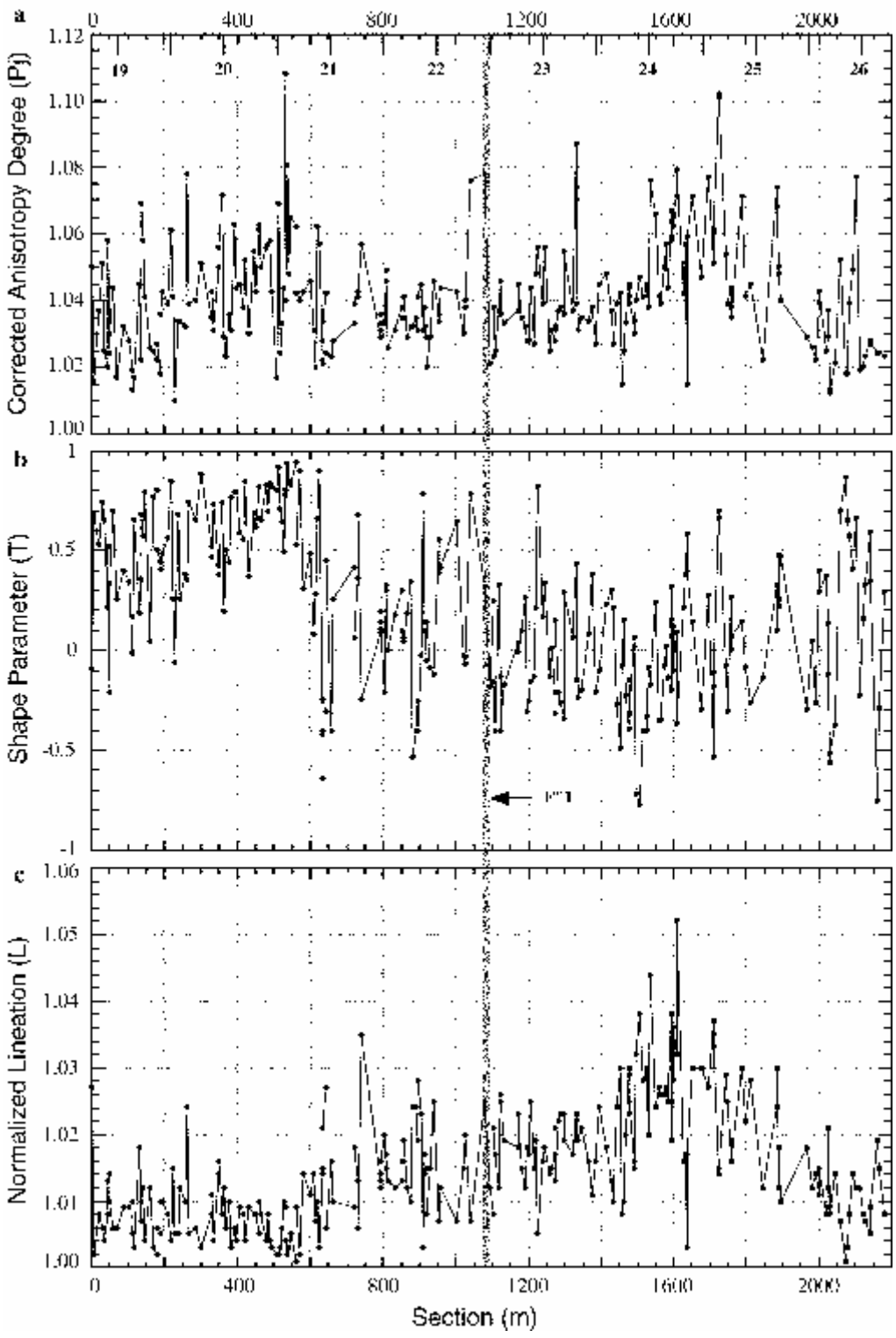

Figure 10. (a) Corrected anisotropy degree (P_j) [*Jelinek*, 1981], (b) shape parameter (T) ($T < 0$ for prolate, pencil-like shapes; $T > 0$ for oblate, pancake-like shapes), and (c) normalized lineation (L) [e.g., *Hrouda*, 1982] plotted against depth (0 is top; 2179 m is bottom). Scale in Ma from correlation II of Figure 5 is provided in Figure 10a.

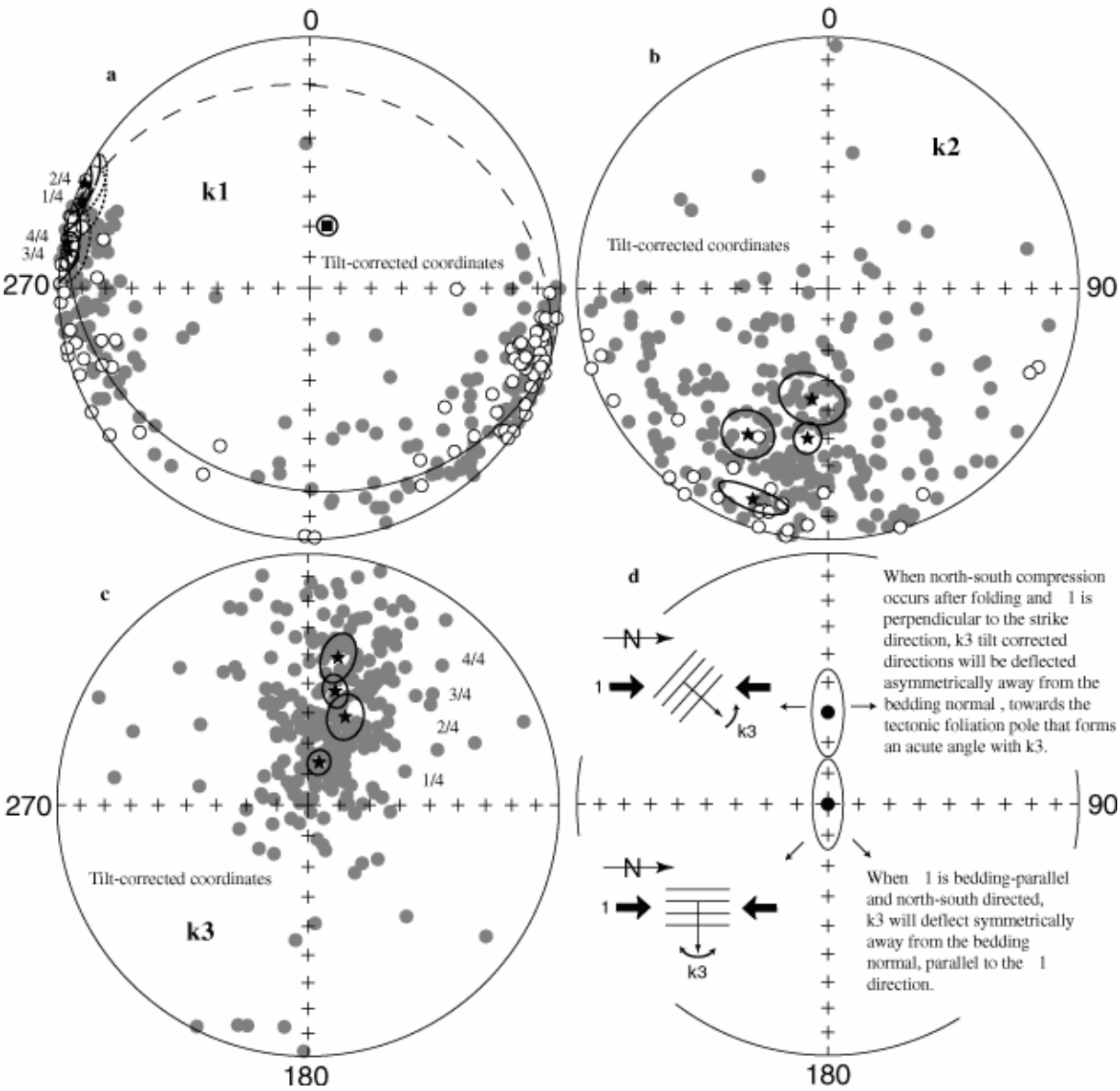

Figure 11. Anisotropy of magnetic susceptibility principal (a) maximum (k_1), (b) intermediate (k_2), and (c) minimum (k_3) directions (all in tilt-corrected coordinates). Figure 11a includes the great circle fit to all the data (pole at D = 15.9°N, I = 69.0°, α_{95} = 3.2°). Figures 11a–11c show the bivariate mean directions [*Henry and LeGoff*, 1995] and 95% confidence ellipsoids for each quarter of the section (1/4 is top; 4/4 is bottom) (Table 2). Note progressive shallowing of k_3 inclinations going from top to bottom of the section. Figure 11d illustrates a model explaining the distribution of the k_3 directions.

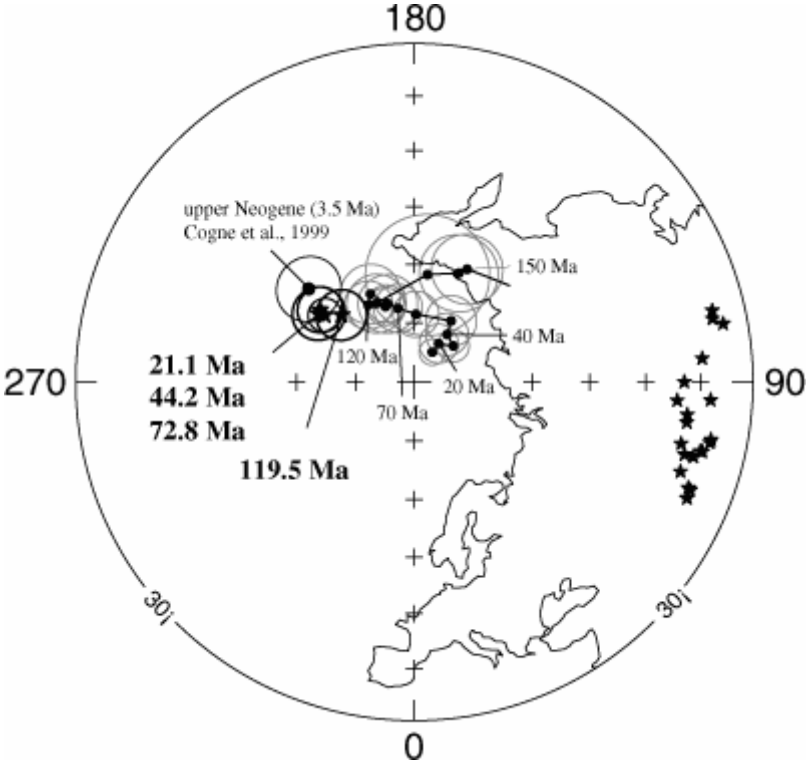

Figure 12. Mean 21.1, 44.2, 72.8, and 119.5 Ma paleomagnetic poles from central Asia (stars) (data from Table 3) together with the Eurasian synthetic apparent polar wander path of *Besse and Courtillot* [1991] (gray circles). Stars on Eurasia are sampling sites from the individual studies from Table 3 and Figure

Tables

Table 1. Summary of Mean Paleomagnetic Directions Used in Magnetostratigraphic Scale and Fold Test[a]

	n	D_g	I_g	D_s	I_s	k	α_{95}
All data	222	355.1	-2.2	350.2	43.8	12.9	2.7
1/4	79	359.1	-2.4			13.1	4.6
1/4	79			359.1	43.3	13.8	4.5
2/4	52	354.5	-4.6	351.8	43.9	12.3	5.9
3/4	60	352.2	1.2			13.1	5.3
3/4	60			341.3	42.9	13.8	5.1
4/4	31	351.6	-3.9			14.0	7.2
4/4	31			342.0	44.3	15.4	6.8
Above F″1	127	357.7	-3.1			12.9	3.6
Above F″1	127			357.0	43.5	13.3	3.6
Below F″1	95	351.6	-0.9			13.2	4.1
Below F″1	95			341.1	43.5	14.4	4.0
Normal only	100	356.2	1.2			13.9	3.9
Normal only	100			352.2	48.2	14.3	3.9
Reverse only	122	174.1	5.0			12.4	3.7
Reverse only	122			168.7	-40.0	12.6	3.7
Site 1[b]	4	47.5	-46.8	153.8	-49.8	16.2	23.6
Site 2[b]	4	177.8	54.8	179.6	-35.0	415.3	4.8
Site 3[b]	4	0.9	-63.7	170.3	-55.1	19.6	22.5
Mean sites 1–3 and n = 222[d]	4	198.4	31.0			1.3	np[c]
Mean sites 1–3 and n = 222[d]	4			349.0	46.4	50.6	13.0

[a]Abbreviations are *n*, number of samples used to calculate mean direction; *D*, declination; *g*, in situ (geographic) coordinates; *I*, inclination; *s*, tilt-corrected (stratigraphic) coordinates (at 100% unfolding); *k*, best estimate of the precision parameter; α_{95}, radius that the mean direction lies within 95% confidence; 1/4, top quarter of section; 4/4, bottom quarter of section, etc.

[b]Data are from *Halim* [1998]; site 1 was recalculated.

[c]Value cannot be precisely estimated.

[d]Magnetostratigraphic section (n = 222) is counted as one site.

Table 2. Anisotropy of Magnetic Susceptibility Principal Axis Directions and Bivariate Statistical Parameters[a]

	n	D_g	I_g	*kx*	*ky*	$\alpha_{95}x$	$\alpha_{95}y$	D_s	I_s	*kx*	*ky*	$\alpha_{95}x$	$\alpha_{95}y$
k_1													
All	262	283.6	-2.9	14.9	4.2	2.2	4.2	284.7	0.5	15.9	4.6	2.2	4.0
1/4	74	281.8	-15.8	25.3	2.9	3.2	9.6	289.2	-2.4	22.2	3.0	3.5	9.5
2/4	60	288.6	-18.3	13.3	5.0	5.0	8.1	295.9	-1.2	16.4	4.6	4.5	8.4
3/4	80	284.6	9.2	22.2	11.9	3.3	4.5	278.8	3.4	20.3	12.5	3.5	4.4
4/4	48	281.7	3.7	12.7	4.0	5.7	10.1	279.9	-1.0	11.0	4.3	6.1	9.7
k_2													
All	262	206.5	80.2	4.9	3.8	3.9	4.5	195.4	33.1	5.2	4.6	3.8	4.0
1/4	74	213.4	53.0	12.3	3.0	4.6	9.5	199.6	11.8	12.8	3.0	4.6	9.4
2/4	60	261.6	68.2	5.8	4.3	7.5	8.7	208.7	34.0	5.4	4.3	7.7	8.7
3/4	80	118.0	81.2	13.6	5.6	4.2	6.6	187.7	39.5	15.1	7.8	4.0	5.6
4/4	48	29.8	74.0	6.5	3.6	7.9	10.6	188.2	53.2	5.7	3.5	8.5	10.8
k_3													
All	262	11.0	11.7	13.4	5.0	2.4	3.9	15.2	59.4	14.1	5.6	2.3	3.6
1/4	74	3.4	30.5	21.7	15.4	3.5	4.1	14.5	75.8	20.1	15.6	3.6	4.1
2/4	60	13.3	10.8	10.0	5.2	5.7	7.9	23.0	58.7	10.0	5.4	5.7	7.8
3/4	80	15.0	3.6	16.4	5.6	3.9	6.6	13.5	51.5	16.5	7.4	3.9	5.7
4/4	48	192.5	11.7	16.2	5.8	5.0	8.4	11.5	39.9	16.9	4.8	4.9	9.2

[a]From *Henry and LeGoff* [1995]. Abbreviations are as in Table 1, with addition of *x* and *y* axis information.

Table 3. Present to Late Jurassic Paleomagnetic Poles From Eurasia, North of the Tibetan Plateau Between 65°E and 105°E Longitude and 34°N and 50°N Latitude[a]

Pole From Figure 1	λ_s	ϕ_s	Age	Age, Ma	λ_p	ϕ_p	A_{95} *dp*/*dm*[b]	*n*	$\lambda_p$smcr	$\phi_p$smcr	Reference; Note
1	34.7	100.7	N2	3.5	66.0	228.6	5.5	9L			*Cogne et al.* [1999]; Jungong
2	38.0	86.5	N1	20	74.4	272.0	4.8/8.0	na	71.8	231.8	*Rumelhart et al.* [1999]; Jianglisai
3	38.5	76.4	E3-N1	21	71.2	226.7	6.7	9L	71.2	226.7	*Chen et al.* [1992]; note age change from K1-2
4	38.1	67.0	E3-N1	21	68.3	238.7	8.3	13L	68.3	238.7	*Chauvin et al*. [1996]; Dekhkanabad
5	39.5	94.7	E3-N1	22.5	69.0	327.8	3.1/5.0	222s	72.5	234.9	this study; Subei
Mean 2–5				21.1			2.8	4S	71.0	233.2	
6	38.1	76.4	E3	30	66.8	210.5	3.4/5.9	na	71.0	231.1	*Rumelhart et al.* [1999]; Aertashi
7	42.3	77.0	E2-3	41	77.5	249.0	6	13L	76.3	229.6	*Thomas et al.* [1993]; Issyk-Kul
8	36.5	102.0	E2	48	61.6	211.3	15.1	5L	70.9	230.8	*Cogne et al.* [1999]; Qaidam
9	37.1	78.4	E2	50	65.3	248.3	4.8/9.0	na	64.4	238.8	*Rumelhart et al.* [1999]; Puksa
10	41.0	71.4	E1-2	52	62.8	291.3	9	9L	67.1	238.2	*Thomas et al.* [1993]; Fergana
Mean 6–10				44.2			4.5	5S	70.0	234.4	
11	37.0	79.0	E1	62	58.1	202.0	12.7	5L	68.3	239.1	*Gilder et al.* [1996]; South Tarim
12	41.2	75.0	E1	62	69.2	241.2	11	16L	69.2	241.2	*Thomas et al.* [1993]; Naryn
13	44.2	86.0	K3-E1	78	73.4	223.1	6.4	9L	73.4	223.1	*Chen et al.* [1991]; South Junggar
14	38.1	76.4	K3	80	71.4	233.6	6.8/11.6	na	71.4	233.6	*Rumelhart et al.* [1999]; Yingjisha
15	42.1	83.2	K3	82	65.9	224.5	9	4L	65.9	224.5	*Li et al.* [1988]; Tarim
Mean 11–15				72.8			3.8	5S	69.8	232.5	
16	39.5	75.0	K1-3	105	70.1	225.8	7	18L	70.1	225.8	*Chen et al.* [1992]; Tarim
17	43.0	90.0	J3-E1	109	65.1	227.8	7	13L	65.1	227.8	*Cogne et al.* [1995]; Turfan
18	38.6	68.9	K	118	82.0	323.0	5	4L	84.5	185.2	*Pozzi and Feinberg* [1991]; Dushanbe
19	36.2	103.5	K1	121	50.3	195.5	4.6	15L	74.0	229.7	*Halim et al.* [1998] (supercedes *Frost et al.* [1995])
20	38.1	66.9	K1	121	66.9	186.1	5	14L	76.2	232.2	*Bazhenov et al.* [1994]; Derbent-A
21	38.1	66.9	K1	121	72.4	214.9	8	9L	72.4	214.9	*Bazhenov et al.* [1994]; Derbent B

22	38.1	68.6	K1	121	81.2	271.8	3	16L	81.1	223.4	*Bazhenov et al.* [1994]; Aksu A
23	38.1	68.6	K1	121	63.6	257.4	17	6L	63.6	239.0	*Bazhenov et al.* [1994]; Aksu B
24	44.2	86.0	J3-K1	129	72.3	227.3	4.8	13L	72.3	227.3	*Chen et al.* [1991]; South Junggar
25	42.0	81.6	J3-K1	129	64.6	208.9	9	6L	70.2	232.0	*Li et al.* [1988]; Tarim
Mean 16–25				119.5			4.3	10S	73.2	227.4	

[a]Abbreviations are λ_s, °N latitude of sampling locality; ϕ_s, °E longitude of sampling locality; Ages are N, Neogene; E, Paleogene; K, Cretaceous; J, Jurassic; 1, Early; 2, Middle; 3, Late; λ_p, °N latitude of pole; ϕ_p, °E longitude of pole; *dp*/*dm* and A_{95}, radius that the mean pole lies within 95% confidence; *n*, number of localities (L), time windows (T), samples (s), or studies (S) used to determine pole; $_p$smcr and $\phi_p$smcr, latitude and longitude of poles rotated by small circles (see text); na, data not available.
[b]Single entries are A_{95} values; double entries are *dp*/*dm* values.